Enhancement of light absorption using high-*k* dielectric in localized surface plasmon resonance for silicon-based thin film solar cells

Hua-Min Li,[1] Gang Zhang,[1] Cheng Yang,[1] Dae-Yeong Lee,[1] Yeong-Dae Lim,[1] Tian-Zi Shen,[1] Won Jong Yoo,[1,a)] Young Jun Park,[2,a)] Hyunjin Kim,[2] Seung Nam Cha,[2] and Jong Min Kim[2]

[1]*Sungkyunkwan University, SKKU Advanced Institute of Nano Technology, 300 Cheoncheon-dong, Jangan-gu, Suwon 440-746, South Korea*

[2]*Samsung Electronics Co., Ltd., San 14-1 Nongseo-dong, Giheung-gu, Yongin 446-712, South Korea*

(Received 23 November 2010; accepted 5 April 2011; published online 10 May 2011)

The application of high-dielectric-constant (k) materials, e.g., Si_3N_4, ZrO_2, and HfO_2, to localized surface plasmon resonance (LSPR) excited by a Au nanoparticle structure has been investigated and simulated for the enhancement of light absorption in Si-based thin film solar cells by using Mie theory and three-dimensional finite-difference time-domain computational simulations. As compared to a conventional SiO_2 dielectric spacing layer, the high-k dielectrics have significant advantages, such as (i) a polarizability over two times higher, (ii) an extinction cross-section 4.1 times larger, (iii) a 5.6% higher transmission coefficient, (iv) a maximal 39.9% and average 25.0% increase in the transmission of the electromagnetic field, (v) an absorption of the transmitted electromagnetic field that is a maximum of 2.8 times and an average of 1.4 times greater, and (vi) increased absorption efficiency and extended cover range. Experimental results show that the average absorptance in the visible spectrum using high-k enhanced LSPR was maximally 31.1% higher than that using SiO_2, demonstrating that the high-k dielectrics can be used as a potential spacing layer for light absorption in Au nanoparticle excited LSPR in Si-based thin film solar cells.
 [doi:10.1063/1.3587165]

I. INTRODUCTION

The physics of surface plasmon excitation have been investigated systematically in recent years. For example, Maier *et al*. reviewed the surface plasmon excitation for the localization of electromagnetic (EM) energy in one, two, and three dimensions.[1] Pitarke *et al*. focused on a theoretical description for various collective electronic excitations at the metal surface.[2] Kuzmiak *et al*. provided a complementary approach for calculating the photonic band structures of EM waves propagating in periodic systems.[3] Sakoda *et al*. and Ito *et al*. demonstrated a numerical simulation of dipole radiation based on the finite-difference time-domain (FDTD) method that provided the accurate dispersion curves, lifetimes, and field distributions of the radiational eigenmodes of photonic crystals, and which is being applied to the investigation of surface plasmon polaritons (SPPs).[4,5]

For the application of the surface plasmon to photovoltaics, Atwater *et al*. reviewed three mechanisms for reducing the physical thickness of the absorbing layer while keeping the optical thickness constant for thin film solar cells: (i) light scattering using localized surface plasmon resonance (LSPR), (ii) light concentration using particle plasmons, and (iii) light trapping using SPPs.[6] LSPR was examined as a promising approach for increasing the energy conversion efficiency of photovoltaic devices,[1,7–9] particularly for thin film hydrogenated amorphous silicon (a-Si:H) solar cells.[10] The LSPR structure effectively decreases the physical thickness of the photovoltaic absorption layer while maintaining a constant optical thickness.[6,8] This is in contrast to other methods such as a pyramidal surface texture,[11] which are unsuitable for thin film devices due to their large-scale feature size as compared to the thickness of the device and the enhanced minority carrier recombination arising from the relatively larger surface area.[6,8] LSPR is frequently excited by EM radiation in proximate metallic nanostructures, which causes selective photon extinction and local EM field enhancement.[12,13] An increase in the short-circuit current density of a-Si:H solar cells was achieved through the enhanced transmission of EM radiation from forward scattering in 50 to 100 nm Au nanoparticles (NPs).[10] An increase in the optical transition rate, which is proportional to the square of the electric field amplitude, enhances the generation of electron-hole (e-h) pairs and increases the photocurrent.

Metallic NP structures are commonly used to excite the LSPR. The dependence of the LSPR on the size, shape, and material of the particle and on the dielectric environment has been studied extensively.[8] SiO_2 (refractive index $n = 1.462$, dielectric constant $\varepsilon = 2.138$ in the visible spectrum)[14] dielectric is the most commonly used spacing layer for realizing LSPR as compared to other dielectrics, e.g., SiC,[15] because it is a good passivation layer, grown easily by thermal oxidation and compatible with most semiconductor fabrication processes. The optimum thickness for LSPR has been reported to be ~25 nm.[16] In comparison, high-dielectric-constant (k) materials, e.g., Si_3N_4 ($n = 2.211$, $\varepsilon = 4.891$ in the visible spectrum), ZrO_2 ($n = 2.179$, $\varepsilon = 4.749$ in the visible spectrum), and HfO_2 ($n = 1.934$, $\varepsilon = 3.740$ in the visible spectrum),[14] showed a red-shift in the LSPR wavelength,

[a)]Authors to whom correspondence should be addressed. Electronic addresses: yoowj@skku.edu and youngjunpark@samsung.com.

and are used as an optional approach for tuning the resonance frequency.[8] Due to the intermediate refractive index between air and Si, they can also be employed as anti-reflection coating (ARC) materials for Si-surface photovoltaic devices.[17] However, the contributions of the high-k dielectrics to light absorption in metallic NP excited LSPR have been unclear so far, and there are few reports of their use in plasmon enhanced photovoltaic applications.

This study investigated the light scattering mechanism theoretically and experimentally, and it examined the use of typical high-k dielectrics as a spacing layer to support Au NP excited LSPR in order to enhance the light absorption in Si-based thin film solar cells. As compared to the conventional SiO_2 dielectric, the relative internal field intensity of a single Au NP with a high-k dielectric spacing layer was increased more than tenfold at the LSPR wavelength. Its polarizability, scattering, absorption, and extinction cross-sections showed a maximum 2.8, 4.7, 2.8, and 4.1 fold increase, respectively, when the spherical radius of the Au NP was 75 nm. According to the Fresnel equations, the transmission coefficient of the high-k dielectric spacing layer was also increased by 5.6%. Based on the three-dimensional FDTD computational simulations, the distribution of the transmitted EM field intensity via the high-k dielectric spacing layer was obtained in both vertical and horizontal directions. Owing to the stronger enhancement of the local field at the LSPR wavelength, the transmission of the EM field intensity showed a maximum increase of 39.9% with a mean increase of 25.0%. Moreover, its absorption in a Si substrate was enhanced by a maximum of 2.8 with an increase of, on average, 1.4 times relative to those using a SiO_2 dielectric. The high-k dielectric spacing layers also improved the absorption efficiency of solar cells and extended their cover range to the longer wavelength region, allowing the use of the near-IR (NIR) region in the solar spectrum. Experimental results showed a 31.1% increase of the average absorptance in the visible spectrum, which is in agreement with our theory and simulation, and which demonstrates significantly enhanced light absorption in the application of Si-based thin film solar cells using Au NP excited LSPR with high-k dielectric spacing layers.

II. THEORY

A. Internal field, polarizability, and dispersion relation

In the quasistatic regime, where the incident wavelength is larger than the particle dimensions, phase shifts or retardation effects of the EM field are negligible, and only dipolar excitations are dominant. Therefore, the internal field E_i of the metallic particle in an external field E_0, which is spatially homogeneous and constant, can be calculated using the electrostatic boundary conditions at the metal-dielectric interface as follows:

$$E_i = E_0 \frac{3\varepsilon_m(\lambda)}{\varepsilon_p(\lambda) + 2\varepsilon_m(\lambda)}, \tag{1}$$

where $\varepsilon_p(\lambda) = \varepsilon_p'(\lambda) + i\varepsilon_p''(\lambda)$ and $\varepsilon_m(\lambda) = \varepsilon_m'(\lambda) + i\varepsilon_m''(\lambda)$ are the wavelength-dependent complex dielectric constants of the metal particle and the dielectric medium, respectively. The E_i of a single Au ($n = 0.824 + i2.600$, $\varepsilon = -6.573 + i3.414$ in the visible spectrum)[14] NP in the quasistatic regime was obtained in SiO_2 and high-k dielectric media, as shown in Fig. 1. At the corresponding LSPR wavelength, the ratio of the internal electric field intensity $|E_i|^2$ to the external electric field intensity $|E_0|^2$ was approximately 5.88 for the SiO_2 dielectric, whereas this value increased significantly to 62.98, 52.12, and 37.01 for the Si_3N_4, ZrO_2, and HfO_2 dielectrics, respectively, which is ten times higher. According to Eq. (1), E_i increases to a maximum when $\varepsilon_p(\lambda) + 2\varepsilon_m(\lambda)$ equals zero. High-k dielectrics have an $\varepsilon_m(\lambda)$ value closer to the $-0.5\varepsilon_p(\lambda)$ of a Au NP than the SiO_2 dielectric, particularly at the corresponding LSPR wavelength, giving rise to a significant increase in the internal field of the Au NP.

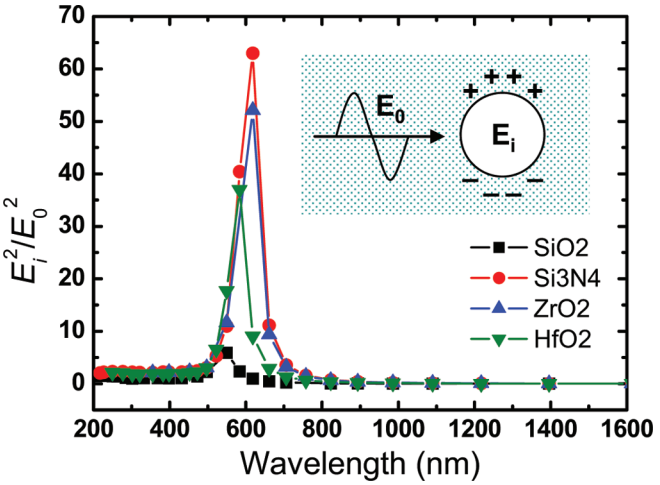

FIG. 1. (Color online) The relative internal field intensity of a single Au NP using SiO_2 and the high-k dielectrics.

According to Mie theory, the polarizability of a particle describes the relative tendency of the charge distribution, e.g., the electron cloud distorted by an external electric field tends to return to the original equilibrium state. Assuming that a spherical metallic particle has a radius of a, its polarizability α can be expressed as[18]

$$\alpha = 4\pi a^3 \frac{\varepsilon_p(\lambda) - \varepsilon_m(\lambda)}{\varepsilon_p(\lambda) + 2\varepsilon_m(\lambda)} = \frac{4\pi a^3[(\varepsilon_p' - \varepsilon_m')(\varepsilon_p' + 2\varepsilon_m') + (\varepsilon_p'' - \varepsilon_m'')(\varepsilon_p'' + 2\varepsilon_m'') + i3(\varepsilon_p''\varepsilon_m' - \varepsilon_p'\varepsilon_m'')]}{(\varepsilon_p' + 2\varepsilon_m')^2 + (\varepsilon_p'' + 2\varepsilon_m'')^2} \tag{2}$$

According to Eq. (2), both the real and imaginary parts, as well as the absolute value of α, were much higher using the high-k dielectrics than using the SiO_2 dielectric, as shown in Fig. 2(a). For example, $|\alpha|$ of a Au NP with $a = 75$ nm showed a peak of 4.57×10^{-20} m^3, 4.22×10^{-20} m^3, and 3.47×10^{-20} m^3 using Si_3N_4, ZrO_2, and HfO_2 dielectrics, respectively, which are approximately 2.8, 2.5, and 2.1 times higher than those obtained using the SiO_2 dielectric

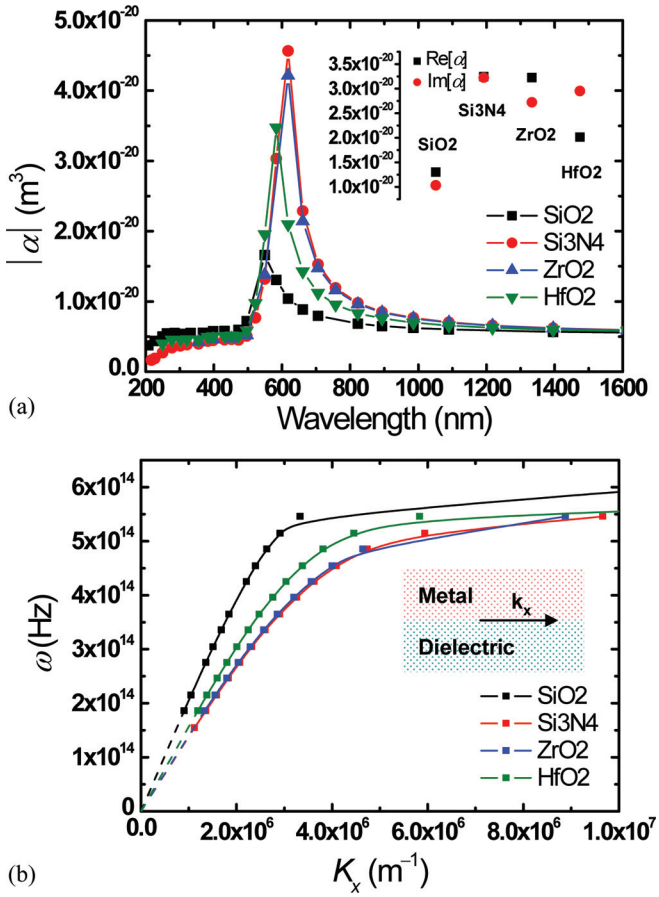

FIG. 2. (Color online) (a) The absolute value of the polarizability of a single Au NP using SiO_2 and the high-k dielectrics. Both the real and the imaginary parts of the polarizability at the corresponding LSPR wavelength are compared in the inset. (b) The dispersion relation for an EM wave propagating at the interface between Au and dielectrics.

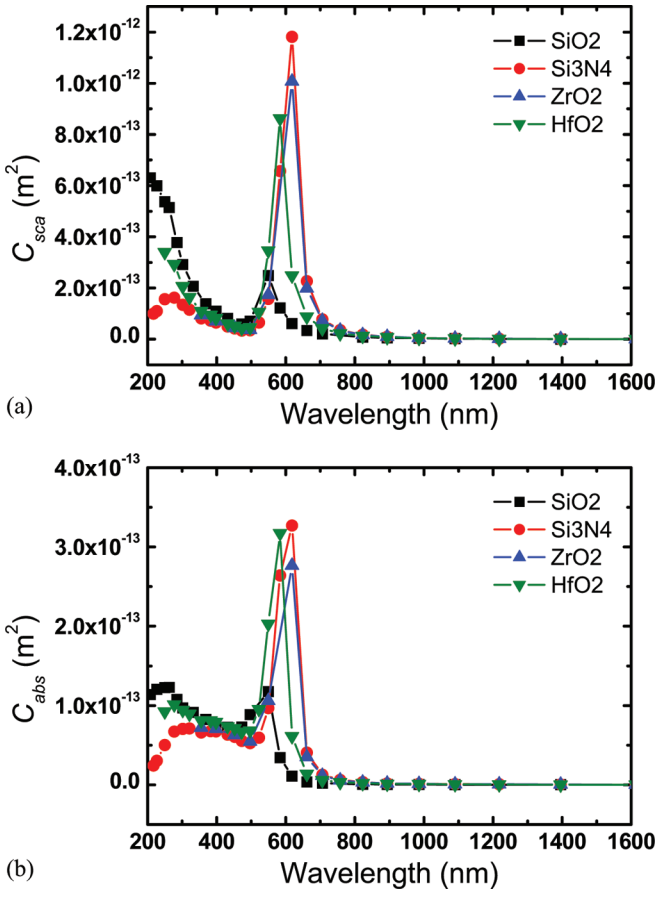

FIG. 3. (Color online) (a) Scattering and (b) absorption cross-sections of a single Au NP ($a = 75$ nm) using SiO_2 and high-k dielectrics. The extinction cross-section as a function of the wavelength is similar to the scattering cross-section due to the dominance of the scattering in the extinction.

$(1.66 \times 10^{-20}\ \mathrm{m}^3)$. Because of the close relevance to light scattering and absorption, the real and imaginary parts of α were also compared at the LSPR wavelength using SiO_2 and the high-k dielectrics, as shown in inset. Moreover, a dispersion relation for the EM wave propagating at the interface between the Au and the dielectrics was obtained, as shown in Fig. 2(b). The wave number at the interface k_x for a surface EM wave was solved based on the following equation:

$$k_x = \frac{\omega}{c}\sqrt{\frac{\varepsilon_p(\omega)\varepsilon_m(\omega)}{\varepsilon_p(\omega)+\varepsilon_m(\omega)}}, \tag{3}$$

where ω is the frequency of the EM wave and c is the speed of light in vacuum. As compared to SiO_2, the high-k dielectrics, e.g., Si_3N_4, ZrO_2, and HfO_2, have a lower surface plasma frequency, indicating a red-shift of the surface plasma resonance in the wavelength. This is in agreement with the previous report.[8]

B. Cross-sections of scattering, absorption, and extinction

Metallic NPs scatter and absorb light to an extreme degree at the LSPR wavelength due to the collective oscillation of the electrons. For a single NP with a diameter well below the incident wavelength, the scattering cross-section C_{sca} and absorption cross-section C_{abs} of a dipole model are defined by the polarizability as follows:[18]

$$C_{sca} = \frac{1}{6\pi}\left(\frac{2\pi}{\lambda}\right)^4 |\alpha|^2 = \frac{8\pi a^6}{3}\left(\frac{2\pi}{\lambda}\right)^4 \left|\frac{\varepsilon_p(\lambda)-\varepsilon_m(\lambda)}{\varepsilon_p(\lambda)+2\varepsilon_m(\lambda)}\right|^2, \tag{4}$$

$$C_{abs} = \frac{2\pi}{\lambda}\mathrm{Im}[\alpha] = 4\pi a^3\left(\frac{2\pi}{\lambda}\right)\mathrm{Im}\left[\frac{\varepsilon_p(\lambda)-\varepsilon_m(\lambda)}{\varepsilon_p(\lambda)+2\varepsilon_m(\lambda)}\right], \tag{5}$$

Light extinction, which is the sum of both scattering and absorption, is described by its corresponding cross-section as $C_{ext} = C_{sca} + C_{abs}$. Due to the greater polarizability at the LSPR wavelength, the C_{sca}, C_{abs}, and C_{ext} of a single Au NP using high-k dielectrics were enlarged significantly, as shown in Fig. 3. For example, the C_{sca}, C_{abs}, and C_{ext} of a single Au NP with $a = 75$ nm using Si_3N_4 dielectric reached a maximum of $1.18 \times 10^{-12}\ \mathrm{m}^2$, $3.27 \times 10^{-13}\ \mathrm{m}^2$, and $1.51 \times 10^{-12}\ \mathrm{m}^2$, respectively, which are approximately 4.7, 2.8, and 4.1 times higher than those obtained using the SiO_2 dielectric, indicating a stronger reaction between the metallic NP and the incident light.

For metallic particles that are much smaller than the wavelength, the extinction in the particle is dominated by the absorption. In this case, the energy is dissipated in heat, which is beneficial to applications such as solar glazing and

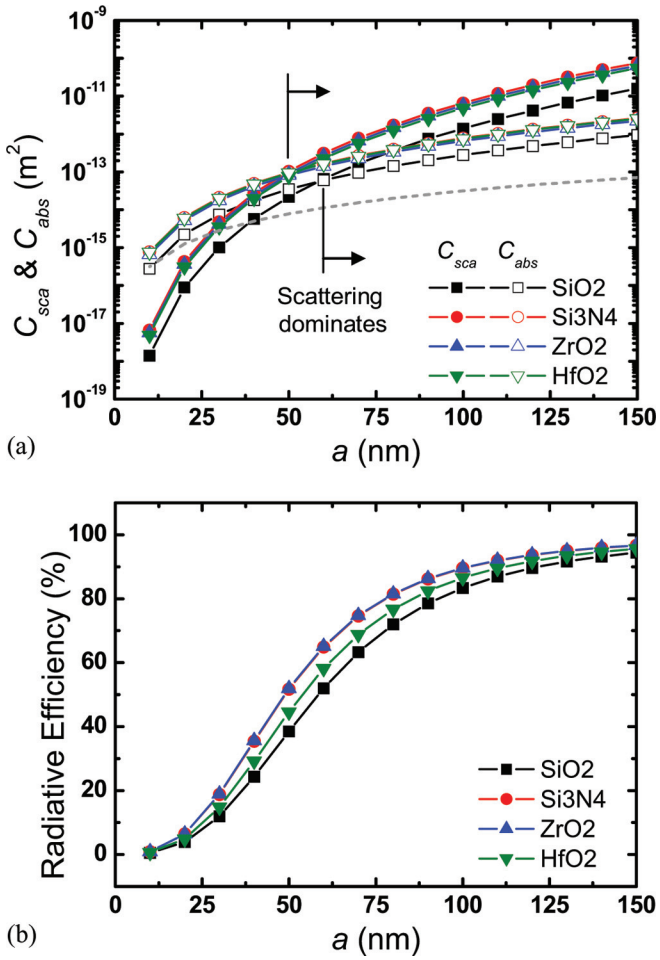

FIG. 4. (Color online) (a) Scattering and absorption cross-sections and (b) the radiative efficiency of a single Au NP as functions of the spherical radius using SiO_2 and high-k dielectrics, as compared to the geometric cross-section (gray dotted line).

nanoscale lithography. In contrast, for the large size metallic particles, the scattering dominates in the extinction, and this is utilized in the application of light trapping in solar cells.[6,8] Therefore, both C_{sca} and C_{abs} using SiO_2 and the high-k dielectrics at the corresponding LSPR wavelength were compared as functions of the radius of the Au NP, as shown in Fig. 4(a). The dominance of the scattering using the SiO_2 dielectric required $a > \sim 60$ nm; this was reduced to ~ 50 nm using the high-k dielectrics. The radiative efficiency or scattering efficiency of Au NPs, which is defined as C_{sca}/C_{ext}, was also obtained, as shown in Fig. 4(b). Using the high-k dielectrics, the radiative efficiency was much higher than that obtained using the SiO_2 dielectric, particularly at a radius of 50 to 100 nm. For example, the radiative efficiency using the ZrO_2 dielectric was 65.1% when $a = 60$ nm, which is higher than that found using the SiO_2 dielectric (52.0%). This indicates that the high-k dielectrics result in a higher proportion of scattering in light extinction, which contributes more to the light trapping in solar cell applications.

C. Scattering direction and transmission coefficient

The scattering of light from a single NP at the LSPR wavelength is mainly in the forward direction.[6,8] According to Mie theory, scattering simulation in SiO_2 and the high-k dielectrics as a function of the scattering direction was obtained, as shown in Fig. 5(a). A forward scattering was confirmed using the high-k dielectrics for the perpendicular, parallel, and natural polarization of light, and values are in agreement with Ebbesen *et al.*'s report.[19] Moreover, the intensity of the scattered light in the high-k dielectrics was about twofold higher than that in the SiO_2 dielectric. This forward scattering results in the transmission of an EM field via the spacing layer, and the transmitted field intensity gives rise to the optical transition rate and the generation of photocurrent in the absorption layer.[10]

A dielectric thin film deposited on a Si surface works as a single-layer ARC and reduces the surface reflection at a certain wavelength. However, due to the existence of the metallic particles, which result in the excitation of the LSPR between the nanoparticle and dielectric, the optical properties, e.g., the reflectance of the particle-dielectric combined layer, become complicated for analysis. In this work, we consider the surface coverage and divide the surface into NP covered and uncovered regions. The NP covered region is dominated by LSPR, and it is analyzed using FDTD simulations in Sec. III. In the NP uncovered region, only the dielectric thin film is considered. According to the Fresnel equations, the transmission coefficient T of the EM field via the spacing layer into the Si substrate was estimated as a function of the incident angle for both s- and p-polarized incident light, as shown in Fig. 5(b). Although the absorption angles were similar, from $-60°$ to $60°$, T through the high-k dielectric spacing layer was higher than that through the SiO_2 dielectric. For example, T values through the air/ZrO_2 and ZrO_2/Si interfaces at the normal incident direction were calculated to be 0.862 and 0.889, respectively, which is in contrast to those through the air/SiO_2 and SiO_2/Si interfaces (0.965 and 0.752, respectively). Assuming negligible energy dissipation and multi-reflection in the spacing layer, T through the ZrO_2 spacing layer was 0.767, which is 5.6% higher than that through the SiO_2 spacing layer (0.726). The higher transmission coefficient indicates an enhancement of the transmitted EM field, leading to a higher optical transition rate and, consequently, increased photogeneration of the e-h pairs.

III. SIMULATIONS

For the proximately spaced NPs, the particle-particle, particle-substrate, and particle-substrate-particle EM interactions complicate the propagation of the transmitted EM field.[10] Therefore, three-dimensional FDTD (Ref. 20) computational simulations were performed in order to estimate the transmitted EM field in the absorbing substrate. In this model, spherical Au NPs were assumed to be arrayed uniformly with a spacing distance of 400 nm so as to reduce the simulation's complexity and processing time. The selected Au NP ($x = 0$ nm, $y = 0$ nm, $z = 75$ nm) with a spherical radius of $a = 75$ nm was located on a Si substrate (-200 nm $< x < 200$ nm, -200 nm $< y < 200$ nm, -2 μm $< z < -30$ nm) with a 30-nm-thick dielectric spacing layer (-200 nm $< x < 200$ nm, -200 nm $< y < 200$ nm, -30 nm $< z < 0$ nm) and illuminated by a

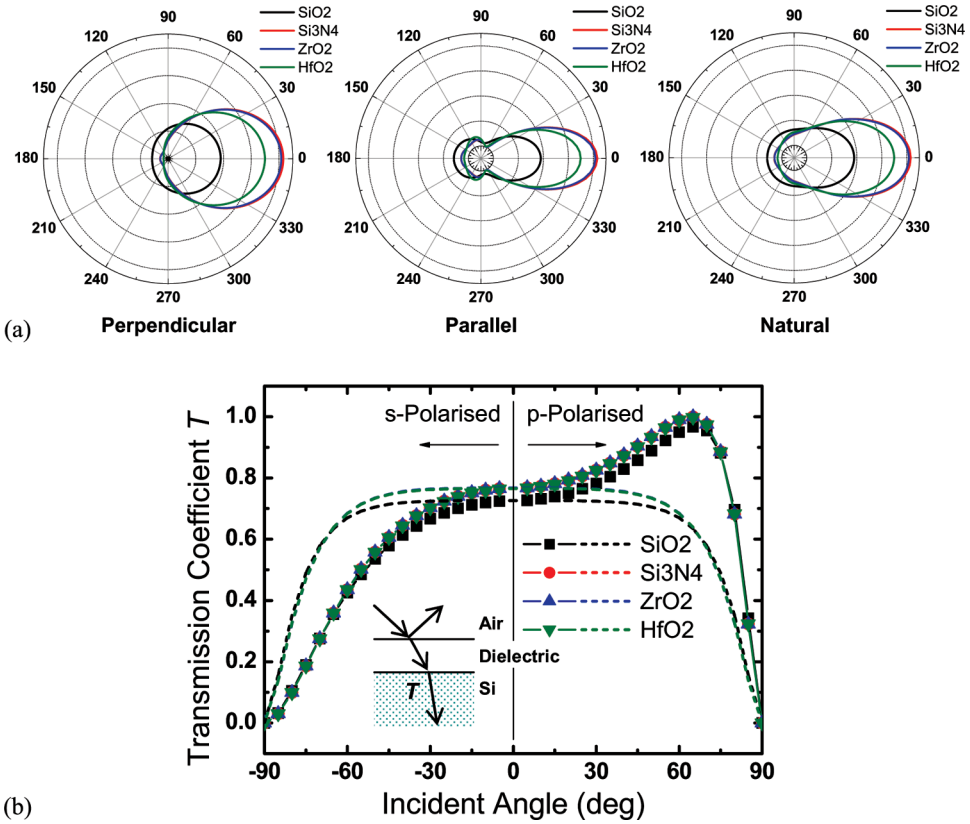

FIG. 5. (Color online) (a) Simulation of Mie scattering as a function of the scattering direction via SiO_2 and the high-k dielectrics for perpendicular, parallel, and natural polarization of light. (b) Transmission coefficient as a function of the incident angle for s-polarized (left side), p-polarized (right side), and unpolarized (dotted line, containing an equal mix of s- and p-polarizations) values via SiO_2 and the high-k dielectric spacing layers.

normal plan wave of air-mass (AM) 1.5 solar spectrum source, as shown in Fig. 6(a). Perfectly-matched-layer boundary conditions were applied, and the mesh size was set to 2 nm for each object and free space. Two monitors were set along the x-z plane (-200 nm $< x < 200$ nm, $y = 0$ nm, -600 nm $< z < -30$ nm) and the x-y plane (-200 nm $< x < 200$ nm, -200 nm $< y < 200$ nm, $z = -500$ nm) in order to observe the vertical and horizontal distributions of the electric field intensity, respectively. Another two parallel monitors were set at the surface (-200 nm $< x < 200$ nm, -200 nm $< y < 200$ nm, $z = 0$ nm) and at a certain depth (-200 nm $< x < 200$ nm, -200 nm $< y < 200$ nm, $z = -600$ nm) in order to observe the volume absorption of the electric field intensity as $|E_t|^2_{(z=0\ \mathrm{nm})} - |E_t|^2_{(z=-600\ \mathrm{nm})}$. Based on these settings, typical distribution profiles of the electric field intensity for both SiO_2 and Si_3N_4 dielectric enhanced LSPR were obtained, demonstrating the existence of LSPR, as shown in Fig. 6(b). The high electric field intensity beside and below the Au NP were arising from the particle SPP resonance and the forward scattering of the incident wave, respectively.[10]

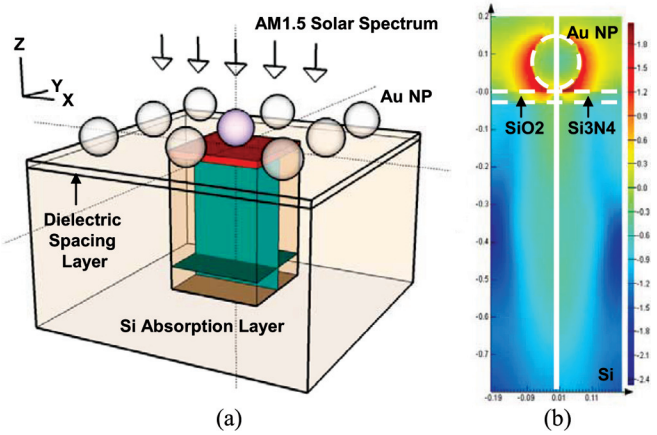

FIG. 6. (Color online) (a) Illustration of the 3D FDTD computational model for simulating the Au NP excited LSPR. The selected Au NP, longitudinal section, transverse section, and absorption volume are also shown for a comparative analysis of SiO_2 and the high-k dielectrics. (b) The distribution profile of the electric field intensity in Au NP excited LSPR using SiO_2 and Si_3N_4 dielectric spacing layers. The diameter of the Au NP is 150 nm, and the thickness of the SiO_2 and Si_3N_4 dielectrics is 30 nm. The wavelength of the incident light source is 550 nm.

A. Distribution of transmitted EM field

The distribution of the transmitted EM field intensity $|E_t|^2$ along the x-z plane via the high-k dielectrics, e.g., Si_3N_4, and the SiO_2 dielectric were observed via the longitudinal section (-200 nm $< x < 200$ nm, $y = 0$ nm, -600 nm $< z < -30$ nm), as shown in Fig. 7(a). The normalized $|E_t|^2$ ($x = 0$ nm, $y = 0$ nm, -600 nm $< z < -30$ nm) via the Si_3N_4 dielectric reached a maximum of ~39.9% (mean ~25.0%) higher than those via the SiO_2 dielectric. This comparison along the x-y plane was also obtained with the transverse section (-200 nm $< x < 200$ nm, -200 nm $< y < 200$ nm, $z = -500$ nm), as shown in Fig. 7(b). For example, the normalized $|E_t|^2$ ($x = 0$ nm, $y = 0$ nm, $z = -500$ nm) via the Si_3N_4 dielectric was ~0.33, which is 37.5% higher than that obtained via the SiO_2 dielectric (~0.24). Other high-k dielectrics, e.g., ZrO_2 and HfO_2, also show similar advantages. The spatial simulations show that both the maximum and the

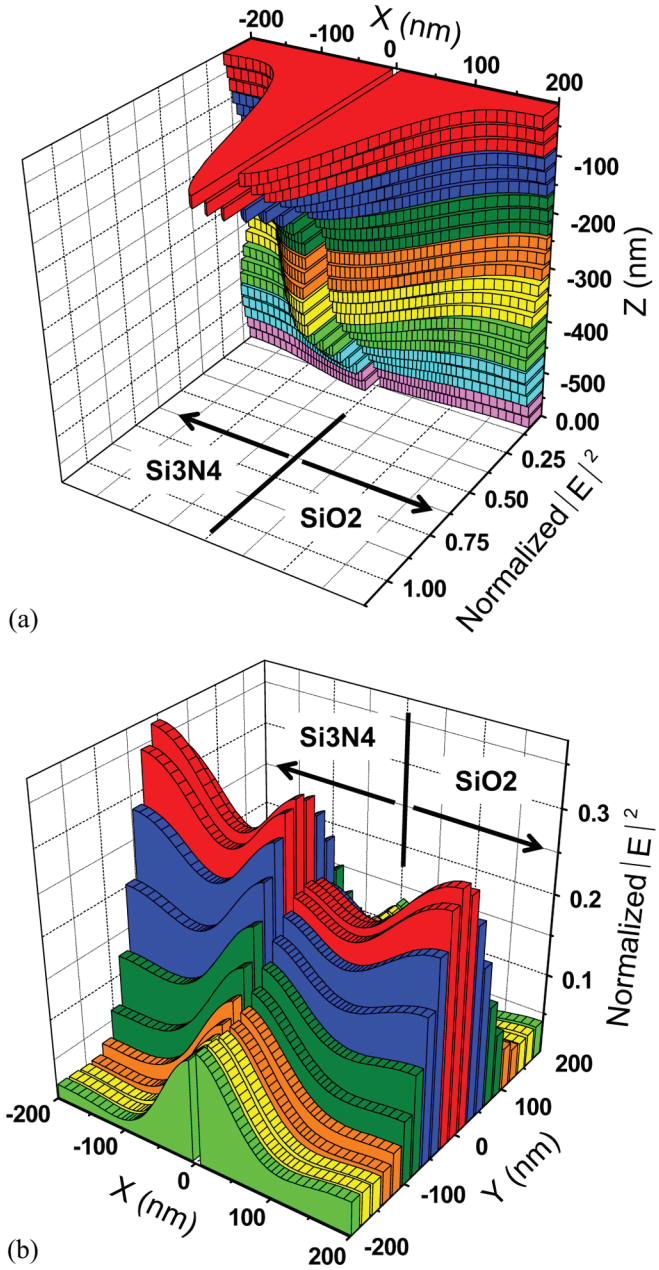

FIG. 7. (Color online) Comparison of the transmitted EM field intensity via the Si_3N_4 (-200 nm $< x < 0$ nm) and SiO_2 (0 nm $< x < 200$ nm) dielectrics along (a) the longitudinal section (-200 nm $< x < 200$ nm, $y = 0$ nm, -600 nm $< z < -30$ nm) and (b) the transverse section (-200 nm $< x < 200$ nm, -200 nm $< y < 200$ nm, $z = -500$ nm).

average values of the transmitted EM field intensity are enhanced significantly using high-k dielectrics, which is consistent with the previous discussion.

B. Absorption of transmitted EM field

The absorption of the transmitted EM field is essential for the photogeneration of charge carriers because the optical transition rate is proportional to the square of the electric field amplitude.[10] In this model, $|E_t|^2$ was measured at the surface ($|E_t|^2_{(z=0\ \text{nm})}$) and at a certain depth in the Si substrate ($|E_t|^2_{(z=-600\ \text{nm})}$). Therefore, the absorption of $|E_t|^2$ in the volume (-200 nm $< x < 200$ nm, -200 nm $< y < 200$ nm, -600 nm $< z < 0$ nm) was obtained as $|E_t|^2_{(z=0\ \text{nm})} - |E_t|^2_{(z=-600\ \text{nm})}$, as shown in Fig. 8(a). At the LSPR

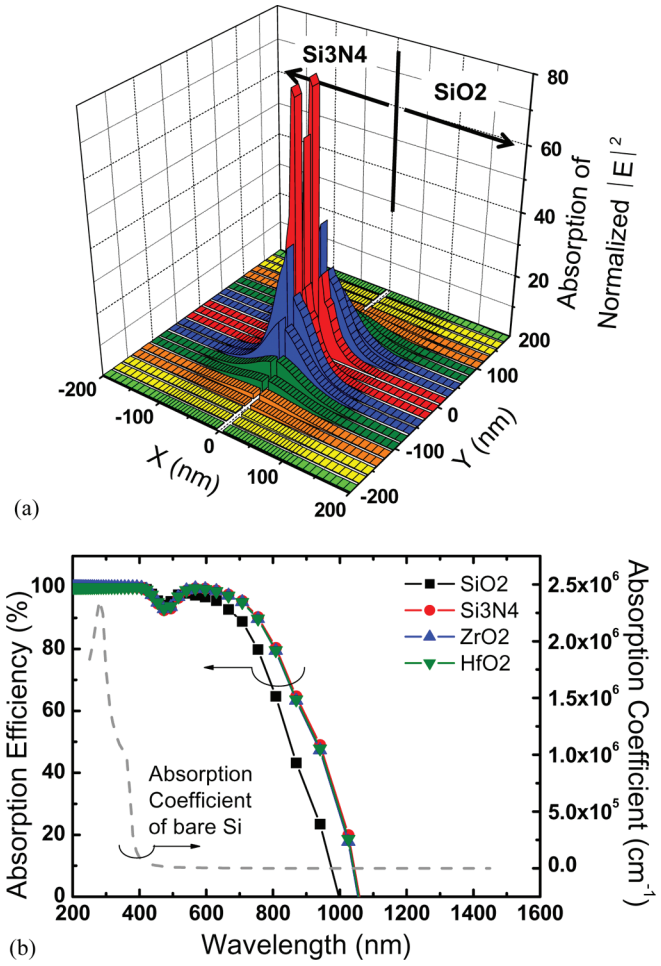

FIG. 8. (Color online) (a) Comparison of the absorption of the transmitted EM field intensity via Si_3N_4 (-200 nm $< x < 0$ nm) and SiO_2 (0 nm $< x < 200$ nm) dielectrics in the volume (-200 nm $< x < 200$ nm, -200 nm $< y < 200$ nm, -600 nm $< z < 0$ nm) of the Si substrate. (b) The absorption efficiency as a function of the wavelength by SiO_2 and the high$-k$ dielectrics. The wavelength dependent absorption coefficient of bare Si is also shown.

wavelength, the normalized absorption of $|E_t|^2$ showed a strong peak at a location below the Au NPs due to the enhanced transmission in the near field. The maximum and average values via the Si_3N_4 dielectric were 78.33 and 2.96, respectively, which are approximately 2.8 and 1.4 times higher than those obtained via the SiO_2 dielectric (28.15 and 2.11, respectively). Other high-k dielectrics, e.g., ZrO_2 and HfO_2, also have similar advantages.

The absorption efficiency, which is defined as $(1 - |E_t|^2_{(z=-600\ \text{nm})}/|E_t|^2_{(z=0\ \text{nm})}) \times 100\%$, was also obtained as a function of the wavelength, as shown in Fig. 8(b). The high absorption efficiency at wavelengths <400 nm was attributed to the high absorption coefficient of Si in the near-UV and middle-UV regions. However, a strong peak at approximately 600 nm resulted from the excitation of near-field plasmons at the LSPR wavelength. When the wavelength differs from the LSPR wavelength, the near-field effect decays considerably, and thereby the absorption efficiency is reduced significantly. According to the simulation results, both the maximum value of the absorption efficiency and the cover range of the wavelength were increased using

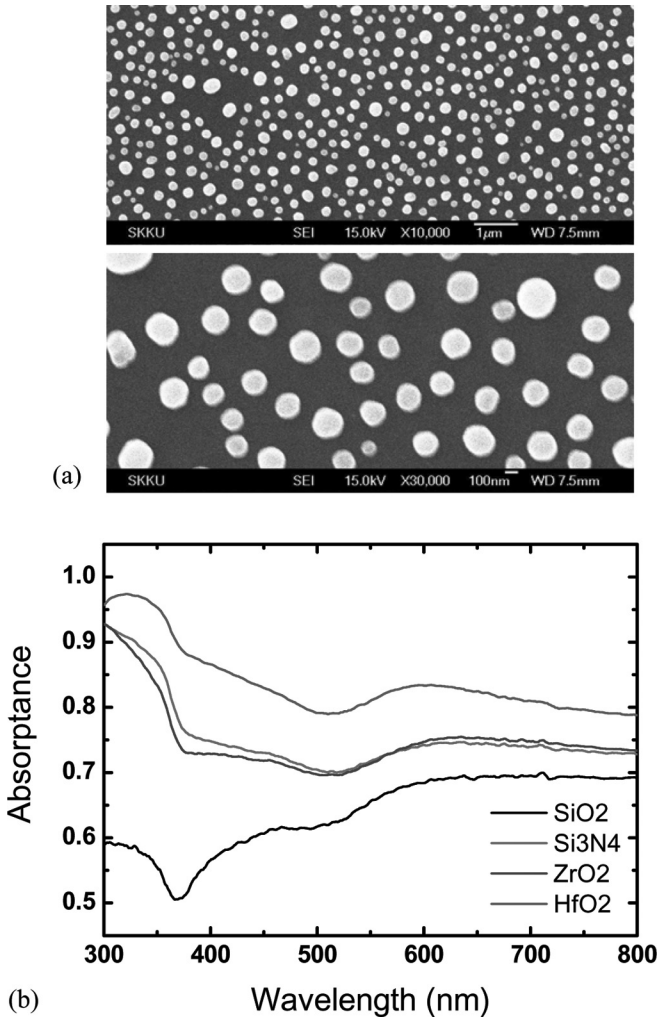

FIG. 9. (a) SEM image of the randomly distributed Au NPs on a SiO_2 surface with an average diameter of 180 to 260 nm. (b) Absorptance using the SiO_2 and high-k enhanced LSPR as a function of the wavelength in the visible spectrum.

the high-k dielectrics. For example, at the corresponding LSPR wavelength, the absorption efficiency was ~99.6% using the high-k dielectrics, which is higher than that obtained using the SiO_2 dielectric (97.9%). Near the corresponding LSPR wavelength, e.g., at 941.2 nm, the absorption efficiency was ~47.8% using the high-k dielectrics, which is more than twice that obtained using the SiO_2 dielectric (23.5%). The wavelength of zero efficiency was also extended to ~1060 nm, as compared to the ~1000 nm obtained using the SiO_2 dielectric, indicating that the high-k dielectric has a wider cover range. As a result, a greater EM field from the long wavelength range, e.g., NIR region, could be absorbed, thereby contributing to the photogeneration of charge carriers.

IV. EXPERIMENTS AND DISCUSSION

First, a p-type polished Si wafer was precleaned as the substrate, onto which 30-nm-thick SiO_2 and high-k dielectrics were deposited via plasma-enhanced chemical vapor deposition and RF sputtering, respectively. Then, a 12-nm-thick Au film was deposited via thermal evaporation, followed by an annealing process in a furnace with a N_2 atmosphere at 400 °C for 50 min. The Au NPs were formed due to the surface tension at high temperature, and their formation is confirmed via scanning electron microscope (SEM), as shown in Fig. 9(a). The average size of the randomly distributed NPs was about 180 to 260 nm, responding equally to any polarizations. It is noted that the physical properties of the high-k dielectrics are sensitive to their fabrication and annealing processes. However, their optical properties still showed a stable performance after a high temperature (over 900 °C for 30 min) annealing test, which was not shown here. Therefore, the annealing effect on the dielectric spacing layer was not considered in this work.

The surface reflectance R of the samples were measured via a UV-Visible spectrometer, and the absorptance A was obtained as $1-R$, as shown in Fig. 9(b). In comparison with the theoretical simulation using the ideal NP, the peak absorptance was not observed at the LSPR wavelength due to the random size distribution and shape of the NPs, which led to a deviation and dispersion of the LSPR wavelength from the theoretical estimation. Even so, the enhancement of the absorptance using the high-k dielectrics was confirmed, and this was consistent with our theory and simulation. For example, the average absorptance in the visible spectrum using high-k enhanced LSPR was about 0.754, 0.749, and 0.838 for Si_3N_4, ZrO_2, and HfO_2, respectively, which is 18.0%, 17.2%, and 31.1% higher than that obtained using SiO_2 (0.639).

V. CONCLUSION

The enhanced light absorption in Au NP excited LSPR using high-k dielectric spacing layers, e.g., Si_3N_4, ZrO_2, and HfO_2, was theoretically and experimentally investigated. As compared to conventional SiO_2 dielectrics, the high-k dielectrics had significant advantages, such as higher polarizability, a larger extinction cross-section, higher transmission and absorption of the EM field, improved absorption efficiency, and an extended cover range. Experimental results show that the average absorptance in the visible spectrum obtained using high-k enhanced LSPR was maximally 31.1% higher than that found using SiO_2, demonstrating that the high-k dielectrics can be a potential spacing layer for light absorption in NP excited LSPR in Si-based thin film solar cells.

ACKNOWLEDGMENTS

This research was partially supported by the Basic Science Research Program through the National Research Foundation of Korea (NRF), funded by the Ministry of Education, Science and Technology (2011-0006268).

[1]S. A. Maier and H. A. Atwater, J. Appl. Phys. **98**, 011101 (2005).
[2]J. M. Pitarke, V. M. Silkin, E. V. Chulkov, and P. M. Echenique, Rep. Prog. Phys. **70**, 1 (2007).
[3]V. Kuzmiak and A. A. Maradudin, Phys. Rev. B **55**, 7427 (1997).
[4]K. Sakoda, N. Kawai, T. Ito, A. Chutinan, S. Noda, T. Mitsuyu, and K. Hirao, Phys. Rev. B **64**, 045116 (2001).
[5]T. Ito and K. Sakoda, Phys. Rev. B **64**, 045117 (2001).
[6]H. A. Atwater and A. Polman, Nature Mater. **9**, 205 (2010).
[7]C. Rockstuhl and F. Lederer, Appl. Phys. Lett. **94**, 213102 (2009).
[8]K. R. Catchpole and A. Polman, Appl. Phys. Lett. **93**, 191113 (2008).

[9]D. M. Schaadt, B. Feng, and E. T. Yu, Appl. Phys. Lett. **86**, 063106 (2005).
[10]D. Derkacs, S. H. Lim, P. Matheu, W. Mar, and E. T. Yu, Appl. Phys. Lett. **89**, 093103 (2006).
[11]S. Fahr, C. Rockstuhl, and F. Lederer, Appl. Phys. Lett. **92**, 171114 (2008).
[12]Y. L. Lu and X. B. Chen, Appl. Phys. Lett. **94**, 193110 (2009).
[13]R. B. Konda, R. Mundle, H. Mustafa, O. Bamiduro, A. K. Pardhan, U. N. Roy, Y. Cui, and A. Burger, Appl. Phys. Lett. **91**, 191111 (2007).
[14]The wavelength-dependent complex dielectric constants for SiO_2, Si_3N_4, ZrO_2, HfO_2, Au, and Si were calculated from their corresponding complex refractive indexes, which were obtained from the Rensselaer Polytechnic Institute, NY, USA, via www.rpi.edu/~schubert/Educational-resources/Materials-Refractive-index-and-extinction-coefficient.pdf.
[15]S. Janz, S. Riepe, M. Hofmann, S. Reber, and S. Glunz, Appl. Phys. Lett. **88**, 133516 (2006).
[16]W. R. Holland and D. G. Hall, Phys. Rev. B **27**, 12 (1983).
[17]P. Singh, S. M. Shivaprasad, M. Lal, and M. Husain, Sol. Energy Mater. Sol. Cells **93**, 19 (2009).
[18]C. F. Bohren and D. R. Huffman, *Absorption and Scattering of Light by Small Particles* (Wiley, New York, 1983).
[19]T. W. Ebbesen, H. J. Lezec, H. F. Ghaemi, T. Thio, and P. A. Wolff, Nature **391**, 667 (1998).
[20]FDTD Solutions (www.lumerical.com).